

Point vortex model for asymmetric inviscid wakes past bluff bodies

Original

Point vortex model for asymmetric inviscid wakes past bluff bodies / Alan, Elcrat; Ferlauto, Michele; Zannetti, Luca. - In: FLUID DYNAMICS RESEARCH. - ISSN 0169-5983. - STAMPA. - 46:3(2014), p. 031407. [10.1088/0169-5983/46/3/031407]

Availability:

This version is available at: 11583/2542514 since: 2017-05-23T22:02:40Z

Publisher:

IOP publishing

Published

DOI:10.1088/0169-5983/46/3/031407

Terms of use:

This article is made available under terms and conditions as specified in the corresponding bibliographic description in the repository

Publisher copyright

(Article begins on next page)

Point vortex model for asymmetric inviscid wakes past bluff bodies

A. Elcrat¹ M. Ferlauto² and L. Zannetti²‡

¹ Mathematics and Statistics Dept., Wichita State University, 1845 Fairmount St, Wichita, KS 67260, USA

² Dept. of Mechanical and Aerospace Engineering, Politecnico di Torino, C.so Duca degli Abruzzi 24, 10129 Turin, Italy

E-mail: Luca.zannetti@polito.it

Abstract. Wakes past bluff bodies are modeled by means of point vortices standing in equilibrium. The consistency of the adopted model is discussed with respect to the asymptotic model proposed by Batchelor. It is shown that, in general, when symmetry is broken, the wake configuration may be neither closed, as for the Batchelor model, nor open, as for the Kirchhoff model. The proposed model has three degrees of freedom, which reduce to one when the locations of separation are prescribed. A further condition has been established for the closure of the wake which reduces the degrees of freedom to zero as for the asymptotic Batchelor model. Existence of multiple solutions, suggestive for real world phenomena, is discussed.

Keywords: Vortex dynamics, Point vortices, Wakes

‡ Corresponding author: luca.zannetti@polito.it

1. Introduction

Wake models for inviscid steady two dimensional flows past bluff bodies are here studied. Batchelor (1956) discussed the asymptotic steady configuration of these flows for the Reynolds number $Re \rightarrow \infty$. He concluded that the wake configuration should be closed and he set his model against the Kirchhoff open-wake model. A schematic of this model, relevant to a symmetric arc-shaped bluff body, is shown in figure 1. The flow is uniform at infinity and is irrotational except inside the finite area wake, which is formed by two vortex patches with opposite-sign vorticity and bounded by vortex sheets.

For uniform flow at infinity, Batchelor (1956) has stated the uniqueness of this steady solution of the Navier-Stokes equations and Chernyshenko (1998) has shown that the vorticity value of the vortex patches and the jump of the Bernoulli constant on the vortex sheets are determined by the location of the separation and by the requirement that the bounding mixing/boundary layers have to be cyclic.

These asymptotic solutions of the Navier-Stokes equations, generally designated as “Prandtl-Batchelor flows”, are peculiar solutions among the infinity admitted by the Euler equations. In fact, from the point of view of purely inviscid flows, an arbitrary distribution of vorticity can be assumed inside a finite area wake for the same far field boundary conditions. For instance, the vorticity can be concentrated on two singularities and the wake can be represented as two bodies of irrotational flow with closed streamlines entrained by two free point vortices. The Batchelor model can then be seen as the extreme of the family of solutions obtained by desingularizing the point vortices into growing vortex patches, as in Elcrat *et al* (2000). The advantage of this model is that the solution can be obtained analytically by classical complex analysis methods. Moreover, on the basis of continuation arguments, such as those used by Gallizio *et al* (2010), relationships can be established between the existence of such point vortex solutions and the existence of the Prandtl-Batchelor solutions.

In his paper, Batchelor (1956) has briefly discussed the case the wake is not symmetric. He had taken for granted that the wake configuration shown in figure 1 is preserved, that is, that the streamlines separating at A and B join at a common point C and enclose a finite area wake internally divided by the streamline DC into two vortex patches. Only symmetry should be lost with the two patches differently shaped.

Below we show that, according to the point vortex model, the scenario for asymmetric wakes is richer. Depending on the value of free parameters, the separating streamlines may not rejoin at a common point C and the wake would then be considered neither closed as for the Batchelor model nor open as for the Kirchhoff model.

Point vortices have been used in modeling incompressible flows for many years, but we mention here some relatively recent works that have tangential relations with what we have to say. For unsteady flows Tang and Aubry (1997) have used unstable modes of Föppl vortices to study transient instabilities of laminar wakes, and de Laet (2007) has used their stable modes to model frequency selection in the vortex shedding regime. The stability of equilibrium positions of point vortices as solutions of a Hamiltonian

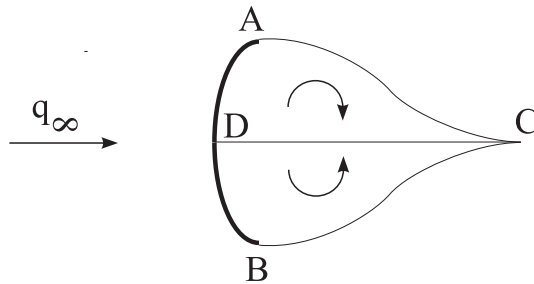


Figure 1. Schematic of Batchelor wake.

system have been studied by Vasconcelos *et al* (2011) and by Shashikanth *et al* (2002). Generally it may be expected that there may be an unstable manifold when there is more than one vortex. In fact, for the Föppl pair it is known that symmetric perturbations are stable and antisymmetric ones are unstable and this used in the work of Tang and Aubry (1997).

Stability of the vortex equilibria found here is an interesting question and we plan to study this question in a subsequent work. However, it should be noted that the stability of the inviscid steady solutions here found have little relevance with respect to the stability of the relevant viscous, high Reynolds number steady solutions, which most likely are unstable for turbulence and Kelvin-Helmholtz instability of separating shear layers, here not taken in account. Nevertheless, regardless of stability, the study of steady inviscid solutions has great importance for flow control purposes. For instance, drag reduction of high Reynolds number flows past bluff bodies requires wake stabilization by some feed-back or passive control mean, which is energetically convenient if operated close to a steady solution, even if unstable.

2. Asymmetric wake past symmetric bodies

Existence of finite area wakes in the flow past arbitrary obstacles protruding from an infinite flat wall has been discussed in Zannetti (2006). It has been shown that, for any geometry, there exists a multi-branched 1D manifold which is the locus of point vortex equilibria pertinent to possible finite area wakes. By assuming the flat wall as a mirror, those solutions are also pertinent to unbounded domains, they result as symmetric solutions past symmetric bodies. Below it is shown that asymmetric flow solutions are also possible. For instance, the Föppl (1913) curve is a branch of the equilibrium manifold pertinent to a semicircular obstacle, thus, it represents a one parameter family of symmetric solutions past a circular cylinder in an unbounded domain. In general, for the same far field boundary conditions, other asymmetric solutions with two standing vortices can be found.

Let $\zeta = \rho \exp(i\varphi)$ be the complex coordinate of the flow field, the general complex potential w for the flow past a unit radius circular cylinder due to a uniform flow at

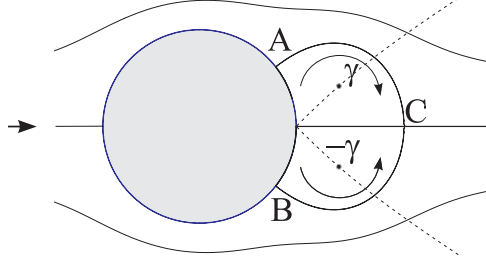


Figure 2. Symmetric Föppl solution, $\gamma_0 = 0$; $\gamma = \gamma_1 = -\gamma_2 = -4.2$.

infinity and two free point vortices is expressed by the equation

$$w = q_\infty \left(e^{-i\alpha} \zeta + e^{i\alpha} \frac{1}{\zeta} \right) + \frac{\gamma_0}{2\pi i} \log \zeta + \sum_{j=1}^2 \frac{\gamma_j}{2\pi i} \log \frac{\zeta - \zeta_j}{\zeta - 1/\zeta_j^*}, \quad (1)$$

where q_∞ and α are the asymptotic velocity and angle of attack, γ_0 is the total circulation, γ_j , with $j = 1, 2$, are the free vortex circulations and (*) denotes complex conjugation. The resulting complex velocity is

$$\frac{dw}{d\zeta} = q_\infty \left(e^{-i\alpha} - e^{i\alpha} \frac{1}{\zeta^2} \right) + \frac{\gamma_0}{2\pi i} \frac{1}{\zeta} + \sum_{j=1}^2 \frac{\gamma_j}{2\pi i} \left(\frac{1}{\zeta - \zeta_j} - \frac{1}{\zeta - 1/\zeta_j^*} \right) \quad (2)$$

and the advection velocities $\dot{\zeta}_j^*$ of the two free vortices are

$$\begin{aligned} \dot{\zeta}_j^* = & q_\infty \left(e^{-i\alpha} - e^{i\alpha} \frac{1}{\zeta_j^2} \right) + \frac{\gamma_0}{2\pi i} \frac{1}{\zeta_j} - \frac{\gamma_j}{2\pi i} \frac{1}{\zeta_j - 1/\zeta_j^*} \\ & + \frac{\gamma_k}{2\pi i} \left(\frac{1}{\zeta_j - \zeta_k} - \frac{1}{\zeta_j - 1/\zeta_k^*} \right), \end{aligned} \quad (3)$$

with $j = 1, 2$ and $k = 3 - j$.

Iosilevskii and Seginer (1994) have done a similar study to detect point vortex equilibria past circular cylinders. They considered the global circulation γ_0 as due to a spinning of the cylinder. In general, different global circulations in the steady flow can be seen as the result of vorticity shed to infinity during different starting transients. Below we show that γ_0 can be determined on a physical basis which leads to multiple flow configurations.

Let the velocity at infinity q_∞ and the cylinder radius R be the reference velocity and length. According to eq. (2), the flow depends on the four real parameters $\alpha, \gamma_0, \gamma_1, \gamma_2$ and on the two complex vortex locations ζ_1, ζ_2 . The equilibrium condition of the free vortices $\dot{\zeta}_1^* = \dot{\zeta}_2^* = 0$, yield four real equations, thus, for a given angle attack α the flow with two standing vortices has three degrees of freedom which can be represented by the values of the circulations $\gamma_0, \gamma_1, \gamma_2$.

The Föppl solutions are pertinent to the choice $\gamma_0 = 0$ and $\gamma_1 = -\gamma_2 = \gamma$, they represent a family of symmetric solutions which depend on the single parameter γ . Non symmetric solutions can be found for different choices of $\gamma_0 \neq 0$ and/or $\gamma_1 \neq -\gamma_2$. For

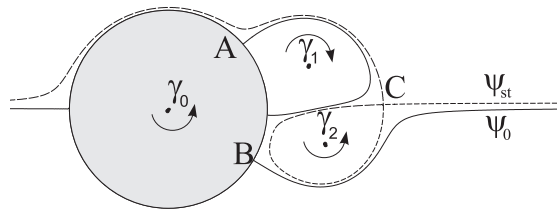


Figure 3. Non-symmetric solution and open wake ($\Delta\psi_{st} \neq 0$) for $\gamma_0 = 0$; $\gamma_1 = -4.7$; $\gamma_2 = 3.7$.

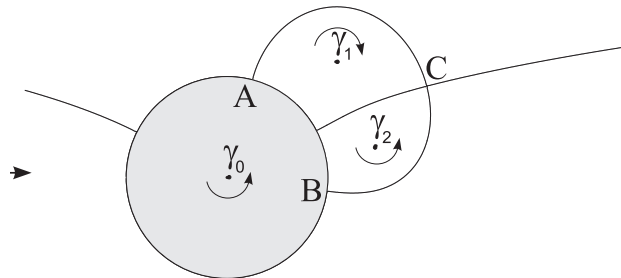


Figure 4. Non-symmetric solution and closed wake ($\Delta\psi_{st} = 0$) for $\gamma_0 = 4.9$, $\gamma_1 = -4.7$, $\gamma_2 = 3.7$.

instance, figure 2 shows the Föppl curves (dotted lines) and the solution for $\gamma = -4.2$ while figure 3 shows the non symmetric solution pertinent to the same $\gamma_0 = 0$ and to $\gamma_1 = -4.7$, $\gamma_2 = 3.7$. These asymmetric solutions and all the other solutions presented throughout the paper have been numerically computed by the Newton method as implemented by the Mathematica (2012) software.

Figure 2 and 3 differ in the value of $\Delta\psi_{st}$ as defined below. Let the wake be defined as the region bounded by the separating streamlines. In the symmetric solution of figure 1, the separating streamlines leave the body surface at points A and B and rejoin at the stagnation point C. They enclose a wake formed by two counter-rotating bodies of fluid entrained by the point vortices. In the non symmetric solution shown in figure 3, the separating streamlines do not rejoin and, as a consequence, the wake is not closed. In fact, while, as above, the streamline separating from point A bounds a region with a clockwise recirculating flow driven by a point vortex, the streamline separating from B extends to infinity and does not bound a flow with closed streamlines. A second counterclockwise rotating flow is embedded in the rear flow, it is bounded by a streamline which presents the stagnation point C and whose stream function value ψ_{st} differs from the solid body value ψ_0 . The stream tube bounded by the streamlines ψ_{st} and ψ_0 is entangled into the wake, from the upper side of the cylinder it is driven to the lower side and then to the downstream infinity. The value of $\Delta\psi_{st} = \psi_{st} - \psi_0$ can be assumed as a measure of the lack of closure of the wake.

The above flows are solutions to the Euler equations. In general, they are not asymptotic solutions of the Navier-Stokes equations for the Reynolds number $Re \rightarrow \infty$ in the form argued by Batchelor (1956). In this respect, the closed wake of figure 2

has some merit, in fact it has the same topology of the Batchelor-flow wake. According to the continuation arguments developed by Gallizio *et al* (2010), the Batchelor-flow wake could be continued onto the above closed wake and vice versa. On the contrary, according to the same reasoning, the open-wake solution of figure 3 holds a weaker physical meaning for it lacks the Batchelor-wake topology and the continuation of the embedded region with closed streamlines into a vortex patch could not be the asymptotic limit for vanishing viscosity for it would violate the maximum principle for vorticity in 2D steady viscous flow as, for instance, discussed by Lugt (1985) and references therein.

By enforcing the closure condition $\Delta\psi_{st} = 0$ the degrees of freedom of the solutions reduces to two. For instance, we can let γ_1 and γ_2 to be free and look for the value of γ_0 which satisfies the closure condition. As an example, figure 4 shows a non symmetric solution with the same values for (γ_1, γ_2) as in figure 3, but with $\gamma_0 = 4.9$ adjusted to obtain a closed wake.

3. Bodies with sharp edges

In the real world of viscous flow, separation is dictated by threshold values of adverse pressure gradients. Moreover, Chernyshenko (1998) has shown that a further constraint to the asymptotic inviscid limit of the separated flow is set by the cyclic nature of the boundary-mixing layer around recirculation regions. It turns out that the inviscid Batchelor model has no degrees of freedom. It should be mentioned here that there are serious issues in carrying out asymptotic analysis for non symmetric problems analogous to that done by Chernyshenko (1998) when there is a single recirculating region or the flow is symmetric. The circulations of the two rotational regions will be different and matching the parameters may be difficult Chernyshenko (2013).

When bodies with two sharp edges are considered, a more physical meaning can thus be provided to the above Euler solutions by reducing the arbitrariness of the choice of free parameters by imposing that separation has to occur at the edges. The above analytical method can then be used by means of conformal mapping and enforcement of two Kutta conditions. The degrees of freedom of the problem are reduced to a single one on physical ground. As argued by Gallizio *et al* (2010), the Batchelor flow solutions should belong to continuations of vortex patches growing from the desingularization of point vortices which satisfy the Kutta conditions.

In figure 5, a circular arc is shown as an example of a body with two sharp edges. The circle arc has been taken on the complex z -plane ($z = x + iy$) with its z_T edges located at $z_T = \pm i$ and its z_V vertex at $z_V = b$ with $\text{Im}(b) = 0$. We assume the velocity at infinity and the half arc chord as reference values for velocity and length, respectively. The Joukowski transformation

$$z = \frac{1}{2} \left(|i - b|\zeta + b - \frac{1}{|i - b|\zeta + b} \right)$$

maps the exterior of the unit circle of the ζ -plane onto the exterior of the z -plane arc. By assuming the ζ -plane as the parameter plane, the complex potential w is still expressed

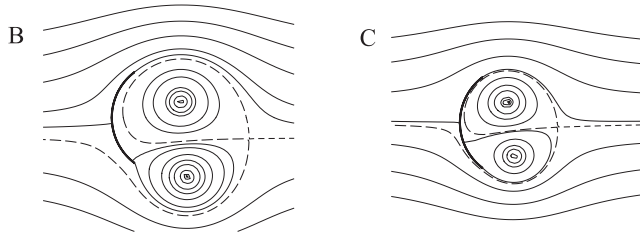


Figure 5. Flows past a circular arc ($\alpha = 0$, $b = -0.5$). **A:** $\gamma_0 = 0$; $\gamma_1 = -7.01$; $\gamma_2 = 7.01$. **B:** $\gamma_0 = 0$; $\gamma_1 = -10.87$; $\gamma_2 = 9.85$. **C:** $\gamma_0 = 0.395$; $\gamma_1 = -7.83$; $\gamma_2 = 7.08$.

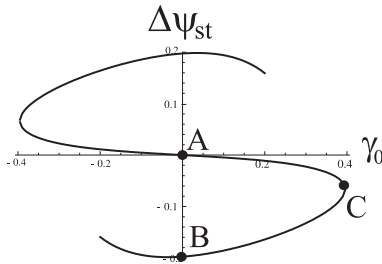


Figure 6. $\Delta\psi_{st}$ versus γ_0 for $\alpha = 0$ and $b = -0.5$.

by the equation (1) where q_∞ is adjusted such that the resulting far field velocity is unit in the physical z -plane, that is, $q_\infty = |i - b|/2$. The complex velocity on the physical plane then is $dw/dz = (dw/d\zeta)/(dz/d\zeta)$. The parameter b defines the radius of curvature R of the arc ($R = -(1 + b^2)/2b$). For $b = 0$ the arc reduces to a flat plate for which, as shown by Smith & Clark (1975), there is not a symmetric solution with two standing vortices which satisfy the Kutta condition. For $b < 0$ such solutions exist, their behavior as b varies has been discussed by Iollo & Zannetti (2003).

According to the Routh rule Clements (1973), vortex equilibrium is expressed by

$$\dot{\zeta}_j^* - \frac{\gamma_j}{4\pi i} \left(\frac{d}{d\zeta} \log \frac{dz}{d\zeta} \right)_{\zeta_j} = 0, \quad (4)$$

where $\dot{\zeta}_j^*$ is expressed by equation (3), with $j = 1, 2$. The Kutta conditions yield the two equations $(dw/d\zeta)_{T_k} = 0$, where $\zeta_{T_k} = (\pm i - b)/|i - b|$, with $k = 1, 2$, are the locations of the edges on the ζ -plane.

For a given incidence α , we assume the free choice of the global circulation γ_0 as the single degree of freedom of the problem. Figure 5 shows a circular arc with $z_V = b = -0.5$. For $\alpha = 0$, solutions exist in the interval $-0.395 \leq \gamma_0 \leq 0.395$. The solutions labeled *A* and *B* are both relevant to $\gamma_0 = 0$, while the solution labeled *C* is relevant the the choice $\gamma_0 = 0.395$. The solution *A* is symmetric with $\gamma_1 = -\gamma_2 = -7.01$; the solution *B* is asymmetric, with $\gamma_1 = -10.87$ and $\gamma_2 = 9.85$; the solution *C* has $\gamma_1 = -7.83$ and $\gamma_2 = 7.08$. No solutions have been found for $|\gamma_0| > 0.395$.

In figure 6, $\Delta\psi_{st}$ is plotted versus γ_0 . The plot terminates at ends beyond which separation/reattachment moves from edge/back-of-the-arc to front-of-the-arc/edge and the wake configuration cannot anymore be considered as physically meaningful. It shows

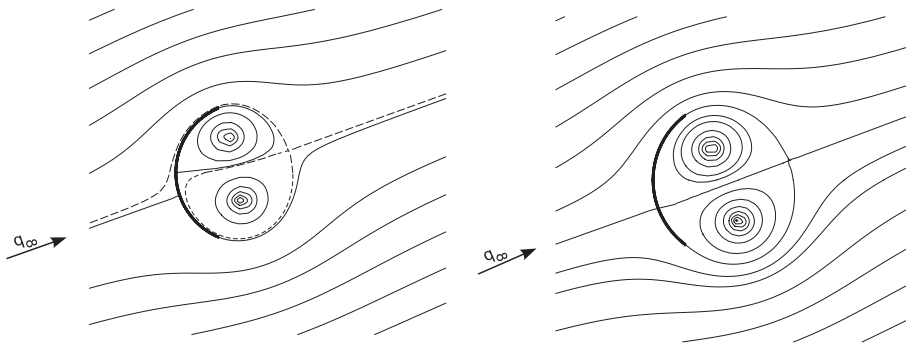


Figure 7. Circular arc at incidence ($\alpha = 20^\circ$). Left: $\gamma_0 = 0$, $\Delta\psi_{st} \neq 0$; right: $\gamma_0 = 0.18$, $\Delta\psi_{st} = 0$

that, for the given incidence $\alpha = 0$ there is a unique value of the global circulation ($\gamma_0 = 0$, solution A) pertinent to $\Delta\psi_{st} = 0$.

Figure 7 presents two solutions for $\alpha = 20^\circ$. On the left, the global circulation is null ($\gamma_0 = 0$) and the wake is open ($\Delta\psi_{st} \neq 0$), while on the right the global circulation has been adjusted ($\gamma_0 = 0.18$) to attain a closed wake ($\Delta\psi_{st} = 0$).

Let us suppose, as argued by Batchelor (1956), that asymptotic wake solutions, symmetric or asymmetric, should be closed, formed by vortex patches with finite area which extend to the solid body boundary. Such solutions “a la Batchelor” could be continued onto closed point-vortex wakes by reducing the vortex patches sizes to vanishing values. By reversing the process, the closed point-vortex solutions assume the special physical meaning of seeds from which inviscid asymptotic solutions could grow. Consequently, the closure condition $\Delta\psi_{st} = 0$ would define a physically meaningful value of the global circulation γ_0 , with a role similar to the Kutta condition in the theory of airfoils.

4. Non circular arcs

Depending on incidence and body shape, there could be multiple solutions which satisfy the $\Delta\psi_{st} = 0$ condition.

Let us consider the asymmetric arc shown in figure 7. It belongs to a two-parameter (c, d) family of arcs whose parametric representation is

$$\begin{aligned} x &= c \sin \vartheta + d \sin 2\vartheta, \\ y &= \cos \vartheta, \end{aligned}$$

with $0 \leq \vartheta \leq \pi$. It is mapped onto a quasi-circle of the λ -plane by

$$\lambda = z + \sqrt{z^2 + 1},$$

and onto the unit circle of the ζ -plane by the Theodorsen-Garrick mapping (see Ives (1976))

$$\lambda = \zeta \exp \left(\sum_{j=0}^{\infty} a_j \zeta^{-j} \right).$$

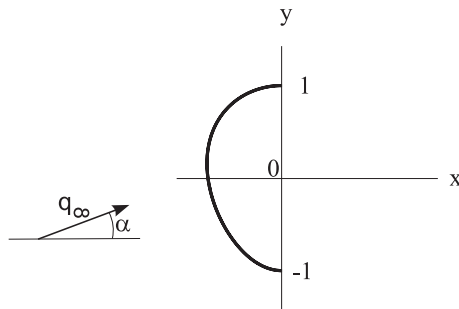


Figure 8. Distorted arc ($c = 0.8$ $d = 0.067$).

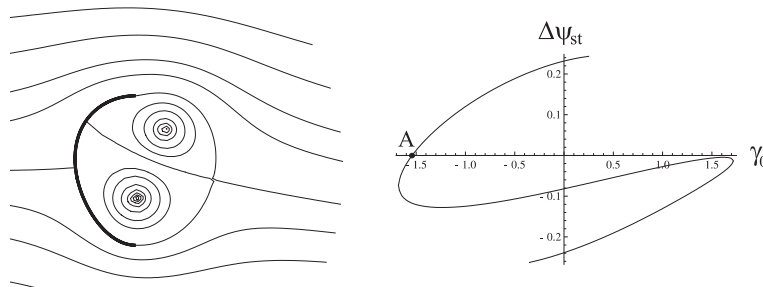


Figure 9. Left: flow field for $\alpha = -5^\circ$, $\gamma_0 = -1.54$. Right: $\Delta\psi_{st}$ versus γ_0 .

Once the series has been truncated at a suitably large value $j = N$, the coefficients a_j are computed according to the method suggested by Ives (1976).

The flow field can be computed following the same procedure as above, with the chain of mappings $\zeta \rightarrow \lambda \rightarrow z$ defining the transformation $z = f(\zeta)$ which maps the exterior of the unit circle of the ζ -plane onto the exterior of the arc of the z -plane.

As examples of wake configurations, we studied the arc shown in figure 8 for two values of incidence, namely, $\alpha = -5^\circ$ and $\alpha = 5^\circ$.

Figure 9 refers to $\alpha = -5^\circ$. On the right-hand side, $\Delta\psi_{st}$ is plotted versus γ_0 . Solutions with two standing point vortices which satisfy the Kutta condition exist in the interval $-1.67 < \gamma_0 < 1.72$. As for figure 6, the curve ends where the flow pattern ceases to be physically consistent. For fixed γ_0 , there can be multiple solutions. The solution with a closed wake (point A, $\Delta\psi_{st} = 0$) is unique ($\gamma_0 = -1.54$, $\gamma_1 = -5.74$, $\gamma_2 = 6.58$), the corresponding flow pattern is shown on the left-hand side of the figure.

As shown in figure 10, when the incidence is varied to $\alpha = 5^\circ$, solutions exist in the interval $-2.11 < \gamma_0 < 1.33$ and the $\Delta\psi_{st}$ curve presents three zeros. In addition to the solution labeled A ($\gamma_0 = -2.07$, $\gamma_1 = -5.36$, $\gamma_2 = 6.48$), homologous to the solution A of figure 9, two other closed wake solutions appear, labeled B ($\gamma_0 = 0.92$, $\gamma_1 = -6.26$, $\gamma_2 = 5.98$), and C ($\gamma_0 = 1.32$, $\gamma_1 = -6.53$, $\gamma_2 = 5.84$). The flow pattern pertinent to the solution B is shown on the left-hand side of the figure. Solution C is a variation close to solution B, while solution A resembles the solution shown in figure 9.

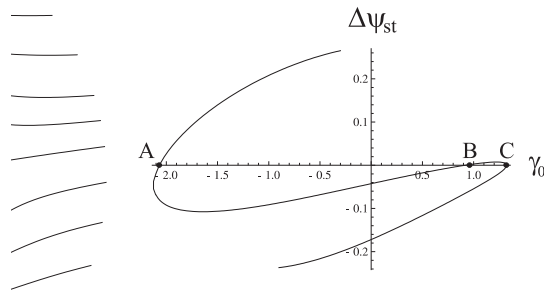


Figure 10. Left: flow field for $\alpha = 5^\circ$, $\gamma_0 = 0.92$. Right: $\Delta\psi_{st}$ versus γ_0 .

5. Force acting on the body

Open or closed apart, the above wakes produce a null drag, $D = 0$, and a lift $L = -\gamma_0 q_\infty$, that is, let X and Y be the x and y components of the resultant force acting on the body, then the Kutta-Joukowski theorem

$$X + iY = -i\gamma_0 q_\infty \exp(i\alpha)$$

holds.

6. Conclusions

The wake past bluff bodies has been modeled by two counter rotating point vortices. When two Kutta conditions are enforced, the problem presents a single degree of freedom, which has been represented by the free choice of the global circulation γ_0 .

In the presented examples, solutions exist for a finite interval of γ_0 .

When the flow is asymmetric, the wake in general is neither a-la-Batchelor closed, nor a-la-Kirchhoff open. A closure condition ($\Delta\psi_{st} = 0$) has been established which determines the value of γ_0 consistent with the wake topology as argued by Batchelor (1956). It reduces the degrees of freedom of the problem to zero.

Examples show that, depending on incidence and body shape, multiple solutions can be found which satisfy the closure condition. This fact could be suggestive for multiple, symmetric and asymmetric steady flow configurations observed in practice in the separated cross flow past rocket bodies, delta wings and aircraft fuselages at high angle of attack, as discussed by Bridges (2010) and references therein.

References

- Batchelor G K 1956 A proposal concerning laminar wakes behind bluff bodies at large Reynolds number *J. Fluid Mech.* **1** 388–398
- Bridges D H 2010 Toward a theoretical description of vortex wake asymmetry *Progr. Aerosp. Sc.* **46** 62–80
- Chernyshenko S I 1998 Asymptotic theory of global separation *Appl. Mech. Rev.* **51** 523–536
- Chernyshenko S I 2013 Private Communication

- Clements R R 1973 An inviscid model of two-dimensional vortex shedding *J. Fluid Mech.* **57** 321–336
- de Laat T W G 2007 Eigenfrequencies of vortex-pair equilibria near an elliptic cylinder or a flat plate in uniform flow *Physical Review E* **75** 036302
- Elcrat A, Forneberg B, Horn M and Miller K 2000 Some steady vortex flows past a circular cylinder *J. Fluid Mech.* **409** 13–27
- Föppl L 1913 Wirbelbewegung hinter einem kreiszylinder *Sitzb. d. k. Baeyr. Akad. d. Wiss., Math-Physi. Klasse, München* **1** 1–17
- Gallizio F, Iollo A, Protas B and Zannetti L 2010 On continuation of inviscid vortex patches *Physica D* **239** 190–201
- Iollo A. and Zannetti L 2003 Trapped vortex optimal control by suction and blowing at the wall *Theor. Comp. Fluid Dyn.* **16** 211–230
- Iosilevskii G and Seginer A 1994 Asymmetric vortex pair in the wake of a circular cylinder *AIAA J.* **32** 1999–2003
- Ives D C 1976 A modern look at conformal mapping, including multiply connected regions *AIAA J.* **14** 1006–1011
- Lugt H J 1985 Vortex flow and maximum principles *Am. J. Phys.* **53**(7) 649–653
- Mathematica 2012 *Mathematica, version 9.0* Wolfram Research, Inc. Champaign, IL
- Shashikanth B N, Marsden J E, Burdick J W and Kelly S D 2002 The Hamiltonian structure of a two-dimensional rigid circular cylinder Interacting dynamically with N point vortices *Phys. Fluids* **14** (3) 1214–1227
- Smith J H B and Clark R W 1975 Nonexistence of stationary vortices behind a two-dimensional normal plate *AIAA J* **13**(8) 1114–1115
- Tang S and Aubry N 1997 On the symmetry breaking instability leading to vortex shedding *Phys. Fluids* **9** (9) 2550–2561
- Vasconcelos G L, Moura N M and Schakel A M J 2011 Vortex motion around a circular cylinder *Phys. Fluids* **23** 126–31
- Zannetti L 2006 Vortex equilibrium in the flow past bluff bodies *J. Fluid Mech.* **562** 151–171